Journal of Chemical Health Risks

www.jchr.org

JCHR (2025) 15(2), 1639-1655 | ISSN:2251-6727

Evaluation of the Accuracy of Multi-Parametric MRI with Adding St-ADC Values in the Detection of Muscle Invasion in Bladder Cancer Using the Vesical Imaging-Reporting and Data System (VI-RADS)

Sarah Mamdouh Osman Ahmed,[1] Noha AbdelShafy ElSaid,[2] Amira Ismail Abdelrahman Mohammed Khater,[3] Waleed Mohamed Mohamed FadlAlla,[4] Mahitab Ibrahim Mohammed Eltohamy,[5] Abeer Ali El-Sharawy,[6] Lobna Mohamed El-Mahdy Bokhary[7]

[1]Lecturer of Radiodiagnosis National Cancer Institute, Cairo University.

[2]Professor of Radiodiagnosis National cancer institute, Cairo university

[3]Lecturer at Cancer epidemiology and Biostatistics department, National cancer instiute, Cairo University.

[4]Lecturer of Oncosurgery National cancer institute- Cairo University

[5]Lecturer of Pathology National cancer institute- Cairo University.

[6]Department of radiology, national cancer instituste, Cairo university.

[7](M.B.B. Ch and MSc) Faculty of Medicine Cairo University

(Received: 16 January 2025 Revised: 20 February 2025 Accepted: 31 March 2025)

KEYWORDS

VIRADS, MRI, bladder cancer, staging, ADC.

ABSTRACT:

Background: Bladder cancer is the 9th most prevalent cancer globally and the 7th in men. Treatment depends on muscle invasion status. Traditionally, staging relies on clinical exams, transurethral resection of bladder tumor specimens (TURB), and imaging. Multiparametric MRI (mp-MRI) is regarded as the optimal imaging for local staging and can complement TURBT. Vesical Imaging-Reporting and Data System (VI-RADS) offers a 5-point scoring system based on various MRI sequences to assess the likelihood of muscle invasion. This study evaluate VI-RADS diagnostic accuracy and the impact of standardized tumor ADC (sT-ADC) values on its sensitivity and specificity.

The aim of the study is to evaluate the accuracy of mp-MRI use (adding sT-ADC values) before TURBT in bladder cancer patients using VI-RADS for discrimination between NMIBC and MIBC.

Materials and methods: This study included 65 patients with suspected bladder cancer who underwent mp-MRI and transurethral biopsy. Two radiologists independently assessed the images. Histopathology confirmed tumor grade and muscle invasion. Statistical analysis evaluated VI-RADS and sT-ADC accuracy for detecting muscle-invasive cancer.

Results: ROC analysis identified a VI-RADS score of ≥3 as the best predictor for MIBC, with 91.5% accuracy, 97.3% sensitivity, and 81.8% specificity (AUC 0.98). For sT-ADC, significant differences were found between NMIBC and MIBC ($p < 0.001$), with 83.7% accuracy at a cut-off of 0.895 (AUC 88.8%). Combining VI-RADS and sT-ADC yielded 100% sensitivity and NPV when results conflicted, and 100% specificity and PPV when both tests agreed.

Conclusion: The Vesical Imaging-Reporting and Data System (VI-RADS) is a thorough scoring system with perfect sensitivity, specificity, and diagnostic value for assessment of deep muscle invasion in bladder cancer cases with a promising add on value regarding the use of ADC in assessment.

Journal of Chemical Health Risks

www.jchr.org

JCHR (2025) 15(2), 1639-1655 | ISSN:2251-6727

Background

Bladder cancer is the 9th most common cancer globally and the 7th most common in men **(1,2).** Its treatment depends on muscle invasion: non-muscle invasive cancer (T1 or lower) is treated with transurethral resection (TURBT) and possibly intra-vesical therapy, while muscle-invasive cancer (T2 or higher) requires radical cystectomy, chemotherapy, radiation, or a combination **(3,4)**. Radical cystectomy carries a high complication rate and decreased quality of life, making accurate preoperative staging crucial **(5).**

Traditionally, staging relies on clinical exams, pathological analysis (via TURBT specimens), and radiologic methods (CT and MRI) to assess metastases. However, TURBT quality varies, and it may miss muscle invasion or cause bladder perforation. This invasive procedure can delay necessary treatment, highlighting the need for more accurate and non-invasive staging methods **(6).**

Multiparametric MRI (mp-MRI), with its superior contrast and recent advancements, is now regarded as the best tool for local staging, complementing rather than replacing TURBT **(6,7).** Mp-MRI offers a faster, non-invasive way to diagnose and stage patients, especially those unfit for surgery. It provides high spatial resolution through T2-weighted imaging (T2WI) for precise anatomical visualization of the bladder wall, while diffusion-weighted imaging (DWI) and dynamic contrast-enhanced MRI (DCE) help identify tumors and distinguish superficial lesions from those invading the muscle layer **(8).**

To standardize mp-MRI in clinical practice, the Vesical Imaging-Reporting and Data System (VI-RADS) was introduced as a 5-point scoring system to assess muscle invasion risk in untreated bladder cancer patients **(9,10).**

Objectives:

Primary objective:

- Evaluation of the accuracy (sensitivity and specificity) of mp-MRI use before TURBT in bladder cancer patients using VI-RADS for discrimination between NMIBC and MIBC.

Secondary objectives:

- Assess the possibility of using MRI as complementary tool with TURBT in the evaluation of cancer bladder patients in the future.
- Assess the concordance between biopsy results and MRI findings.
- Assess rate of up staging to muscle invasive disease.

Materials and methods

This prospective study included 65 cases from two different hospitals (50 cases from the first one and 15 cases from the second), referred by the uro-surgery department to the uro-radiology unit.

Study Population:

Between November 2019 and July 2021, 65 patients with suspected urinary bladder cancer underwent mp-MRI.

Clinical trial number:

Not applicable

Inclusion criteria:

- Patients having urinary bladder mass detected on Ultrasound (U/S) and/or CT examinations.

Exclusion criteria:

- Patients who received treatment (Chemotherapy, radiotherapy, BCG or operative treatment as TURBT).
- Patients with contraindications to MR imaging (e.g. pacemaker, metallic prostheses, claustrophobic patients).
- Refusal to consent to the study.

• All 65 patients underwent transurethral cystoscopic biopsy following MR imaging (1- 4 weeks), and six patients who showed at MR variable degree of mural thickening and intra luminal lesions of the urinary bladder were confirmed as negative for bladder carcinoma (their histology results showed benign conditions i.e. cystitis, prostatitis and benign prostatic hyperplasia). The tumor was histologically confirmed in the remaining 59 patients, of whom 5 had multiple lesions. Specifically, 3 patients had 2 lesions, 1 patient had 2 lesions, and 1 patient had 3 lesions. Total number of malignant lesions was about 70 lesions.

Journal of Chemical Health Risks

www.jchr.org

JCHR (2025) 15(2), 1639-1655 | ISSN:2251-6727

MRI technique:

• The patients were fasting 6 hours before examination, administered intra-muscular antispasmodic agent and instructed to drink 500-1000 ml of water in 30 minutes before the examination in order to obtain adequate distension of the bladder. In case of presence of a urethral catheter, 250–400 ml of sterile saline was used to distend the bladder.

• MRI was performed on high field system (1.5 Tesla) closed magnet unit (Phillips Achieva XR) using Torso coil (16 channel) and Siemens Aira (1.5 Tesla). All the patients were imaged in the supine position, adequacy of bladder distension and correct position of the coil were checked on localizer images, and the examination was postponed if the bladder was not adequately distended.

Imaging Protocol:

A urinary bladder focused protocol **(Table 1)** with high-resolution images and high signal-to-noise ratio (SNR) compatible with VI-RADS scoring was used in both hospitals. Localizer sequences are used to verify proper positioning of the surface coil, ensure sufficient bladder distension, and plan the coverage for the initial high-resolution imaging sequences.

A suitable field-of-view (FOV) was chosen to encompass the entire bladder along with adjacent structures, including pelvic lymph nodes, the proximal urethra, pelvic bones, the prostate, and seminal vesicles in male patients, as well as gynecological organs in female patients.

T2 WI:

2D fast-spin-echo (FSE) T2WI or PROPELLER T2-weighted sequences (3–4 mm) sequences are acquired employing a small FOV and a large matrix, in three orthogonal planes (axial, coronal, and sagittal). The choice of the optimal imaging plane, which is typically the one most perpendicular to the bladder wall under evaluation, is largely determined by the tumor's location. This approach ensures accurate visualization of the tumor's relationship with the bladder wall and perivesical fat while reducing partial volume artifacts.

Diffusion-weighted imaging (DWI):

DWI was performed using free-breathing spin-echo echo-planar imaging (EPI) with spectral fat suppression in two perpendicular planes (axial and either sagittal or coronal). To generate an apparent diffusion coefficient (ADC) map, at least two b-value sequences were used, with one of the b-values being in the range of 500–1000 s/mm² to provide adequate contrast resolution relative to the surrounding tissues.

Dynamic contrast enhancement (DCE):

Single injection of Gadovist administered at a dose of 0.1 mmol/kg at a rate of 3 ml/s.
During the early injection phase (<60 seconds), the mucosa and submucosal layers (inner layers) demonstrate enhancement and appear with high signal intensity (SI) compared to the relatively hypoenhancing bladder muscle (outer layer), which exhibits low SI. Images are obtained 30 seconds after contrast injection, followed by 4–6 additional acquisitions at 30-second intervals. This timing helps detect the early enhancement of tumors and mucosa, as well as any tumor extension into the hypointense muscle layer, which typically enhances later (~20 seconds vs. ~60 seconds after contrast administration, respectively). Delayed phase acquisitions are not necessary for urinary bladder cancer staging due to the reduced SI contrast between the different wall layers and the tumor, as well as the presence of high SI contrast agent excreted into the bladder lumen.

Image interpretation:

All cases from both institutes were assessed and the scoring was conducted independently by two uroradiologists, who had 15 and 10 years of experience in radiology, respectively. They assigned a VI-RADS score to each patient to evaluate the risk of detrusor muscle invasion, without knowledge of surgical or histologic results.

Any discrepancies between the two reviewers were resolved through discussion and consensus.

T2 WI: was the first sequence to be interpreted in which the integrity of the muscularis propria appearing as a continuous low signal line was assessed. The inner layer couldn’t be assessed in this sequence as it elicits same signal as that of urine (high signal).

Journal of Chemical Health Risks

www.jchr.org

JCHR (2025) 15(2), 1639-1655 | ISSN:2251-6727

DCE: the tumor and the intact inner layer showed early post-contrast enhancement while the intact detrusor muscle showed late enhancement. Absent early enhancement of the inner muscle layer suggests its infiltration. Interruption of enhancement of low signal of deep muscle layer suggests its infiltration.

DWI:

a- Qualitative assessment:

- This was done by studying the signal intensity of different lesions on both the DWIs (at the highest b value i.e. at 1000 sec/mm2) and the ADC map.

- The lesions usually elicited high signal (in higher b-values) with corresponding low ADC signal whilst the tumor stalk and inner muscle layer elicits low signal intensity.

b- Quantitative assessment:

- Due to technical factors such as insufficient spatial resolution and motion during scanning, accurate ADC measurement was hindered in 10 patients out of 59 ones, even with good DWIs, so ADC was measured in only 49 patients.

- A ROI was manually set in to maximally cover the index tumor on a transverse ADC map at the MRI section of the largest tumor diameter, or the ROI was placed 3 times when possible and then the mean ADC value for the lesion was calculated.

- ADC values were measured for the gluteus maximus muscle as well with a ROI of area 5 cm^2 set within it.

- A standardized tumor ADC (sT-ADC) was calculated by dividing the mean tumor ADC value by the mean gluteus maximus ADC value to account for the incompatibility between different MRI protocols.

Histo-pathologic analysis:

The hematoxylin–eosin stained slides from biopsies were examined for histopathologic diagnosis, stage, and muscle invasion. Grading was based on cellularity, nuclear features, and mitotic activity. Low-grade urothelial carcinoma shows delicate papillae and orderly cells with minimal mitosis, while high-grade urothelial carcinoma displays fused papillae, disordered cells, nuclear atypia, pleomorphism, and active mitoses. A specimen is classified as high grade if it contains at least 5% of high-grade components.

Statistical analysis

A total sample size of 59 bladder cancer cases will be needed to provide a two-sided 95% confidence interval for a single proportion using the large sample normal approximation with confidence limits 8%. This number will be increased by 10% to account for expected losses, so the total number needed will be 65 bladder cancer cases. Sample size estimation was performed by Epi Info 7 statistical package.

Data management and analysis were performed using Statistical Package for Social Sciences (SPSS) vs. 21. Age was summarized using median and range. Categorical data were summarized as numbers and percentages. The associations between the VI-RADS scores as well as its components and the pathologic muscle-invasion status were evaluated using chi square test for linear trend. Comparisons of the two pathologic invasiveness groups (muscle invasive & non-muscle invasive) regarding ADC and sT-ADC were done using Mann-Whitney tests.

The receiver operating characteristic (ROC) curve analysis and area under the ROC curve (AUC) were used to assess the VIRADS and sTADC scorings' abilities to detect a muscle-invasive tumor. The diagnostic performance of the dichotomized VI-RADS as well as sT-ADC scores for detecting muscle-invasive tumors were evaluated by the calculation of sensitivity, specificity, positive predictive value, negative predictive value and accuracy. P-values < 0.05 were considered significant.

Important statistical definitions:

- **Sensitivity:** Reflects proportion of lesions categorized as muscle invasive lesions upon the radiological method out of all pathologically proven MIBC lesions.

- **Specificity:** Reflects proportion of lesions categorized as non-muscle invasive lesions upon the radiological method out of all pathologically proven NMIBC lesions

- **Positive predictive value:** proportions of radiologically scored lesions as muscle invasive and pathologically proven to be muscle invasive.

Journal of Chemical Health Risks

www.jchr.org

JCHR (2025) 15(2), 1639-1655 | ISSN:2251-6727

- **Negative predictive value:** proportions of radiologically scored lesions as non-muscle invasive and pathologically proven to be non-muscle invasive

Figure titles and legends

Case1: Fig. 2: Conventional non-enhanced axial T2 WI (a), DCI (b), DWI {b values 1000} (c) and ADC map (d). Internal stalk (red arrow)

➢ **History and clinical data**: A 44-year-old male, presented with painless hematuria.

➢ **MRI findings and VI-RADS scoring:**

● **Conventional MRI (T2 WI):** Two exophytic polypoidal soft tissue lesions are seen projecting form the left and right lateral walls of the urinary bladder. The largest one is seen on the left side measures about 2.2 x 2.6 cm in its maximum axial dimensions, elicits high T2 WI signal intensity with internal low signal stalk. Intact low T2 WI signal of the detrusor muscle is seen. **(VI-RADS 2)**

● **DCI:** Heterogeneous post-contrast enhancement in the early dynamic phases with internal non-enhancing low signal stalk. No evidence of neither interruption nor early enhancement of the deep muscle layer. **(VI-RADS 2)**

● **DWI** The lesion shows high signal intensity in all b values, with internal low signal stalk. **(VI-RADS 2)**

▪ **Final score: VI-RADS 2.**

● **ADC map** The lesion shows relatively low signal intensity with mean ADC values of the most restricted ROIs about 0.82×10^{-3} mm^2/s. The mean ADC value of the Gluteus maximus muscle was 0.54×10^{-3} mm^2/s.

▪ **sT-ADC: 0.82 / 0.54 = 1.51 (> the cutoff value 0.895)**

➢ **Pathology:** Transitional cell carcinoma, low grade with intact muscularis propria (NMIBC).

● **The lesion of greater burden was radiologically suggested to be non-muscle invasive based on both VI-RADS scoring and ADC values which was confirmed pathologically to be NMIBC.**

● **Case 2: Fig. 3:** Conventional non-enhanced axial T2 WI (a), DCI (b), DWI {b values 1000} (c) and ADC map (d).

➢ **History and clinical data**: A 63-year-old male, presented with painless hematuria.

➢ **MRI findings and VI-RADS scoring:**

● **Conventional MRI (T2 WI):** An exophytic sessile soft tissue lesion is seen projecting form the right posterior wall of the urinary bladder seated on the right vesico-ureteric junction with consequent mild backpressure changes, measures about 1.5 x 3 cm in its maximum axial dimensions. It elicits high T2 WI signal intensity with intact low T2 WI signal of the detrusor muscle seen. **(VI-RADS 3)**

● **DCI:** Homogenous post-contrast enhancement in the early dynamic phases. No evidence of inner layer enhancement. No evidence of neither interruption nor early enhancement of the deep muscle layer. **(VI-RADS 3)**

● **DWI** The lesion shows high signal intensity in all b values. **(VI-RADS 3)**

▪ **Final score: VI-RADS 3.**

● **ADC map** The lesion shows relatively low signal intensity compared to pelvic muscles with mean ADC values of the most restricted ROIs about 0.58×10^{-3} mm^2/s. The mean ADC value of the Gluteus maximus muscle was 0.76×10^{-3} mm^2/s.

▪ **sT-ADC: 0.58 / 0.76 = 0.76 (< the cut off value 0.895)**

➢ **Pathology:** Transitional cell carcinoma, high grade with infiltrated muscularis propria (MIBC).

● **Case (3) Fig. 4:** Conventional non-enhanced axial T2 WI (a), DCI (b), DWI {b values 1000} (c) and ADC map (d)

➢ **History and clinical data**: A 69-year-old female, presented with painless hematuria.

➢ **MRI findings and VI-RADS scoring:**

● **Conventional MRI (T2 WI):** An exophytic sessile soft tissue lesion is seen projecting form the right posterior wall of the urinary bladder, measures about 1.5 x 2 cm in its maximum axial dimensions eliciting

Journal of Chemical Health Risks
www.jchr.org
JCHR (2025) 15(2), 1639-1655 | ISSN:2251-6727

iso/high T2 WI signal intensity with intact low signal of the detrusor muscle. **(VI-RADS 3)**

- **DCI:** Homogenous post-contrast enhancement in the early dynamic phases. No evidence of inner layer enhancement. No evidence of neither interruption nor early enhancement of the deep muscle layer. **(VI-RADS 3)**

- **DWI:** The lesion shows high signal intensity in all b values. **(VI-RADS 3)**

- **Final score: VI-RADS 3.**

- **ADC map :**The lesion shows relatively low signal intensity compared to pelvic muscles with ADC value of the most restricted ROI about 0.59×10^{-3} mm^2/s. The mean ADC value of the Gluteus maximus muscle was 0.36×10^{-3} mm^2/s.

- **sT-ADC: 0.59 / 0.36 = 1.6 (> the cut off value 0.895)**

➢ **Pathology:** Transitional cell carcinoma, low grade with spared muscularis propria (NMIBC).

➢ **The lesion was radiologically equivocal regarding VI-RADS scoring being of score 3, however its ADC value raised the possibility of being non-muscle invasive, which was confirmed pathologically to be NMIBC.**

Case (4) Fig. 5: Conventional non-enhanced axial T2 WI (a), DCI (b), DWI {b values 1000} **(c)** and ADC map (d). Focal areas of interruption of low signal muscularis propria (red arrow)

➢ **History and clinical data**: A 61-year-old male, presented with hematuria and burning micturition.

➢ **MRI findings and VI-RADS scoring:**

- **Conventional MRI (T2 WI):** An exophytic sessile/flat soft tissue lesion is seen projecting form the left lateral and posterior walls of the urinary bladder with encroachment upon the left vesico-ureteric junction and associated ipsilateral mild backpressure changes. It measures about 2.1 x 7.4 cm in its maximum axial dimensions eliciting high T2 WI signal intensity with focal areas of interruption of low signal muscularis propria however with no definite extra-vesical extension. **(VI-RADS 4)**

- **DCI:** Homogenous post-contrast enhancement in the early dynamic phases with focal areas of interruption of the deep muscle layer. **(VI-RADS 4)**

- **DWI:** The lesion shows high signal intensity in all b values with focal areas of encroachment upon the deep muscle layer **(VI-RADS 4)**

- **Final score: VI-RADS 4.**

- **ADC map** The lesion shows low signal intensity compared to pelvic muscles with ADC value of the mean of most restricted ROIs about 0.67×10^{-3} mm^2/s. The mean ADC value of the Gluteus maximus muscle was 0.76×10^{-3} mm^2/s.

- **sT-ADC: 0.67 / 0.76 = 0.881 (< the cut off value 0.895)**

➢ **Pathology:** Transitional cell carcinoma, Grade 3 with the first partial TURBT showed spared muscularis propria (NMIBC), while the completion TURBT done after one month showed infiltration of deep muscle layer (MIBC).

➢ **The lesion was radiologically suggested to be muscle invasive according to the VI-RADS scoring and ADC values, which was confirmed pathologically to be MIBC in the 2nd completion TURBT.**

Case (5) Fig. 6: Conventional non-enhanced axial T2 WI (a), DCI (b), DWI {b values 1000} (c) and ADC map (d). Interruption of the deep muscle layer and focal area of extra-vesical extension (red arrow).

➢ **History and clinical data**: A 61-year-old male, presented with painless hematuria.

➢ **MRI findings and VI-RADS scoring:**

- **Conventional MRI (T2 WI):** An exophytic flat soft tissue lesion is seen projecting form the left lateral wall of the urinary bladder showing maximum thickness about 1.2 cm eliciting iso T2 WI signal intensity with interruption of the deep muscle layer and focal area of extra-vesical extension. **(VI-RADS 5)**

- **DCI:** Homogenous post-contrast enhancement in the early dynamic phases with interruption of the deep muscle layer and focal area of extra-vesical extension. **(VI-RADS 5)**

Journal of Chemical Health Risks

www.jchr.org

JCHR (2025) 15(2), 1639-1655 | ISSN:2251-6727

- **DWI:** The lesion shows high signal intensity in all b values with interruption of the deep muscle layer and focal area of extra-vesical extension. **(VI-RADS 5)**

- **Final score: VI-RADS 5.**

- **ADC map** The lesion shows low signal intensity compared to pelvic muscles with ADC value of the most restricted ROIs about 0.65×10^{-3} mm^2/s. The mean ADC value of the Gluteus maximus muscle was 0.77×10^{-3} mm^2/s.

- **sT-ADC: 0.65 / 0.77 = 0.844 (< the cut off value 0.895)**

➢ **Pathology:** Transitional cell carcinoma, Grade 3 with infiltration of deep muscle layer (MIBC).

➢ **The lesion was radiologically suggested to be muscle invasive according to the VI-RADS scoring and ADC values, which was confirmed pathologically to be MIBC.**

Results

Patient demographics:

Fifty-nine patients were included in this study, 50 of them were males and 9 were females, their ages ranged from 0 to 92 years (median age 61).

The most common clinical symptoms were painless hematuria and fullness in the lower abdomen found in 51 patients (86.4%).

Among the 59 patient, 47 patients only had single tumors while 5 patients had multiple tumors with total number of 70 lesions. The highest score lesions were the ones considered.

Demographics of the lesions:

About 1/3 of lesions were seen involving the trigone and lateral walls of the urinary bladder with the majority (about 78%) having exophytic pattern of growth. About 54.2 % were papillary while 27.1 % were sessile while the rest were of mixed shape. All of the lesions were >1cm size.

Histopathological analysis:

All 59 patients underwent transurethral cystoscopic biopsy within 1–4 weeks, confirming malignancy. Most lesions (91.5%) were transitional cell carcinoma, 6.8% squamous cell carcinoma, and the rest non-small cell carcinoma. High-grade lesions accounted for 49.2%, moderate-grade 27.1%, and the rest low-grade. Muscle invasion was present in 62.7%, with 36 undergoing radical cystectomy, while 37.3% were non-muscle invasive, and 20 had TURBT. Three patients were lost to follow-up.

Radiological analysis:

Radiological assessment and VI-RADS scoring of lesions were based on T2, DWI, and DCE imaging **(Figure1)**. Most lesions (76.3%) showed high T2 signal with 22% of the cases with internal stalk **(Figure 2)**, 94.9% had restricted diffusion in DWI, and 81.4% exhibited homogenous post-contrast enhancement in DCE. The inner layers of 88.1% of lesions were not visible in T2WI/DWI and non-enhancing in DCE **(Figures 3 & 4)**, suggesting their infiltration. The detrusor muscle was interrupted in 49.2% of lesions with extra-vesical extension **(Figure 5**), while 10.2% had interruptions only without extra vesical extension **(Figure 6)**, and the rest were preserved

VI-RADS scoring:

The scores of VI-RADS and the three-image series of the mp-MRI for the detection of muscle invasion by the bladder lesions were summarized in **(Table 2).**

In a study of 59 patients, 37.3% had non-muscle-invasive cancer and 62.7% had muscle-invasive cancer. No bladder tumors were scored as VI-RADS 1. For muscle-invasive tumors, the VI-RADS scores were 1 (1 tumor), 2 (1 tumor), 3 (6 tumors), 4 (6 tumors), and 5 (29 tumors). Chi-square tests showed a significant linear relationship (P, .001) between T2, DW, and CE imaging and VI-RADS scores, indicating that higher VI-RADS scores correlate with increased muscle invasion.

Prospective validation of VI-RADS score in NMIBC and MIBC differentiation before TURBT

The VI-RADS scoring system for distinguishing NMIBC and MIBC before TURBT showed high sensitivity and specificity. With a cut-off of ≥3, sensitivity was 97.3%, specificity 81.8%, PPV 90%, and NPV 94.7% **(Table 3)**. Raising the cut-off to ≥4 decreased sensitivity (94.6%) but increased specificity (100%) and both PPV and NPV to 100% and 91.7%,

Journal of Chemical Health Risks

www.jchr.org

JCHR (2025) 15(2), 1639-1655 | ISSN:2251-6727

respectively with overall accuracy 96.6% **(Table 4)**. ROC analysis showed that a VI-RADS score ≥3 had the best performance for detecting MIBC with an AUC of 0.98 **(Figure 7)** and overall accuracy of 91.5%**.**

Fig. 7: ROC curves for VI-RADS scoring and sT-ADC.

Accuracy of ADC values to detect MIBC

Due to technical limitations, ADC values were only measured for 49 of the 59 patients **(Table 5)**. In 49 of 59 patients, tumor ADC values ranged from 0.37 to 1.7 × 10−3 mm²/s. MIBC patients had significantly lower values (median 0.65) than NMIBC patients (median 0.76). The sT-ADC values also differed significantly between the groups. ROC analysis for sT-ADC detection of MIBC showed an AUC of 88.8, with a cut-off of 0.895 **(Figure 7)** yielding 83.3% sensitivity, 84.2% specificity, and 83.7% accuracy **(Table 6)**.

Fig. 7: ROC curves for VI-RADS scoring and sT-ADC.

Combination of VI-RADS and ADC values to detect MIBC:

When there was a conflict between VI-RADS scores and sT-ADC values in predicting muscle invasion (e.g., VI-RADS ≥3 or sT-ADC ≤0.895), the sensitivity and NPV were both 100%. This was also true for a VI-RADS cut-off value of ≥4. When both VI-RADS and sT-ADC values agreed in predicting muscle invasion (e.g., VI-RADS ≥3 and sT-ADC ≤0.895), the specificity and PPV were 100%, which was consistent with a VI-RADS cut-off of ≥4. In clinical practice, ADC values can help refine diagnosis by emphasizing muscle invasion in VI-RADS 4 and 5 lesions, excluding it in VI-RADS 2 lesions, and guiding staging in equivocal VI-RADS 3 lesions **(Table 7)**.

Discussion

This study evaluated the effectiveness of the VI-RADS scoring system and mp-MRI in assessing muscle invasion in bladder cancer (BCa). Our results indicated that all lesions scored as VI-RADS 4 and 5 were confirmed as muscle-invasive upon pathological examination, achieving 100% accuracy, which is in line with findings from previous studies **(5, 11)**. To a large extent, similarly, **(12)** reported that all VI-RADS 5 lesions were muscle invasive, and 86.11% of VI-RADS 4 lesions were muscle invasive. These results support the high diagnostic accuracy of VI-RADS scores 4 and 5 in detecting muscle invasion.

Our results for VI-RADS 4 and 5 lesions closely align with those of **(13)** who reported high percentages of muscle invasiveness for scores 4 and 5 across seven readers with varying experience levels. Their findings ranged from 68.2% to 96.2% for score 4, and 92% to 100% for score 5.
One case in our study demonstrated the potential for false negative results and understaging with primary partial TURBT, which initially indicated a non-muscle invasive lesion. However, VI-RADS scoring of the lesion as VI-RADS 4 suggested muscle invasion, which was confirmed by a second TURBT one month later. This highlights the importance of pre-operative mp-MRI and VI-RADS scoring in predicting muscle invasion, particularly for large lesions. Using mp-MRI can reduce the need for multiple cystoscopies, avoid delays in diagnosis, and minimize patient exposure to invasive procedures. Additionally, mp-MRI can help guide surgeons to the most likely areas of muscle invasion for biopsy during the initial TURBT.

Our study showed that tumors scored as VI-RADS 2 were predominantly non-muscle invasive, with 94.7% of the lesions confirmed as non-muscle invasive, which is consistent with studies by **(5)** and **(12)**, which reported 95.2% and 95.08% non-muscle invasive lesions for VI-RADS 2, respectively.

VI-RADS 3 lesions in our study had a higher rate of non-muscle invasive tumors (80%), which agrees with studies by **(15)** and **(14)** showing 91.4% and 100 % of VI-RADS 3 lesions as non-muscle invasive, though (5) found 66.7% of VI-RADS 3 lesions to be muscle invasive. This variability highlights the challenges in relying solely on the VI-RADS 3 score to predict muscle invasion.

Regarding the ROC analysis, we found that a VI-RADS cutoff value ≥3 had an AUC of 0.98 (95% CI: 0.94–1), with sensitivity of 97.3%, specificity of 81.8%, PPV of 90%, and NPV of 94.7% and over all accuracy of 91.5%, suggesting that VI-RADS can well reflect the muscle-invasive condition when the VI-RADS score is ≥ 3 with high statistical significance of p-value <0.001. These findings align with those of **(16)**, who showed a sensitivity of 91.2% and specificity of 78.8%, and **(17)**, who reported an AUC of 0.83 with a sensitivity of 78%,

Journal of Chemical Health Risks

www.jchr.org

JCHR (2025) 15(2), 1639-1655 | ISSN:2251-6727

specificity of 88% PPV 78%, NPV 88% and over all accuracy 84% with high statistical significance as p-value <0.001. A meta-analysis **(18)** also found similar results, with pooled sensitivity of 0.87 and specificity of 0.86 for a cutoff ≥3.

Our study found that using sT-ADC alone with a cutoff of 0.895 for detecting muscle invasion had lower accuracy compared to VI-RADS scoring, with an AUC of 88.8%, sensitivity of 83%, and specificity of 84.2%, compared to the AUC of 98.2%, sensitivity of 97.3%, and specificity of 81.8% for VI-RADS scoring. These findings were similar to those of previous studies, such as **(19)**, which showed a slight decrease in accuracy using sT-ADC alone compared to VI-RADS scoring.

When combining VI-RADS ≥3 and sT-ADC < 0.895, specificity improved to 100%, eliminating false positives. However, this led to under-staging 20% of cases as non-muscle invasive, increasing false negatives, with a sensitivity of 80%. This result aligns with (19), where specificity improved from 70% to 97%, but sensitivity decreased from 78% to 61%.

Our study showed that when there was a conflict between VI-RADS scoring and sT-ADC values, prioritizing the higher tumor burden (VI-RADS ≥3 or sT-ADC < 0.895) resulted in 100% sensitivity, detecting all muscle-invasive lesions, though specificity dropped to 68.2%, leading to 31.8% over-staging. This finding is consistent with (19), which reported an increase in sensitivity from 78% to 100% and a decrease in specificity from 70% to 53% when using the same criteria.

These results emphasize the importance of ADC as a functional biomarker for differentiating MIBC from NMIBC, with potential to improve muscle invasion detection in higher VI-RADS lesions, and to guide staging of equivocal lesions. However, further studies with larger sample sizes are needed to validate the addition of ADC values to the VI-RADS scoring system.

Additionally, mp-MRI showed potential in follow-up for NMIBC patients, detecting small recurrent lesions, which could reduce the need for invasive cystoscopy. However, post-surgical changes in MRI may pose challenges, which could be overcome using DCE-MRI and DWIs, as demonstrated in other studies **(20)**.

Our study underscores the importance of incorporating ADC values alongside VI-RADS scoring to enhance diagnostic accuracy, especially in equivocal cases. It also emphasizes the potential of mp-MRI in reducing the need for multiple cystoscopies, particularly in follow-up care.

Limitations:

There are some limitations in our study that warrant mentioning;

1. Conducting the study in tertiary referral hospitals limited early-stage (VI-RADS 1) cases.

2. The small sample size led to fewer cases in certain categories, like VI-RADS 3.

3. CIS, a high-risk type, is difficult to assess with mpMRI.

4. Using 1.5T MRI scanners reduced detail compared to 3T scanners.

Recommendation:

1. Studies on larger sample sizes are needed to support the importance of ADC values in the VI-RADS scoring system.

2. The role of VI-RADS in following up patients after TURBT needs to be reinforced as it would play an important role in decreasing invasive follow up cystoscopy procedure especially for those patients who are incompatible to cystoscopy as those unfit for anesthesia or with urethral stricture.

Conclusion

Our study proved the great effectiveness of the Vesical Imaging-Reporting and Data System (VI-RADS) as a thorough scoring system with perfect sensitivity, specificity, and diagnostic value for assessment of deep muscle invasion in bladder cancer cases, with a promising add on value regarding the use of ADC in assessment

We suggest using VI-RADS scoring for assessment of muscle invasion in bladder cancer cases pre-operatively but with cautious interpretation for lesions scored as VI-RADS 2 and 3.

Journal of Chemical Health Risks

www.jchr.org

JCHR (2025) 15(2), 1639-1655 | ISSN:2251-6727

LIST OF ABBREVIATIONS

Apparent Diffusion Coefficient	(ADC)
Area under the curve	(AUC)
Bladder cancer	(BCa)
Carcinoma in-situ	(CIS)
Computerized tomography	(CT)
Confidence Interval	(CI)
Contrast-enhanced	(CE)
Diffusion Weighted MRI	(DW MRI)
Dynamic Contrast Enhanced MRI	(DCE MRI)
Echo-planar imaging	(EPI)
Fast spin-echo	(FSE)
Field of view	(FOV)
Fluid Attenuation Inversion Recovery	(FLAIR)
Gradient echo	(GRE)
Intravesical Bacillus Calmette–Guerin	(BCG)
Magnetic resonance imaging	(MRI)
Methotrexate, Vinblastine, Doxorubicin/Adriamycin, Cisplatin	(MVAC)
Multiparametric MRI	(mp-MRI)
Muscle invasive bladder cancer	(MIBC)
National Cancer Institute	(NCI)
Negative Predictive Value	(NPV)
Non-muscle invasive bladder cancer	(NMIBC)
Positive Predictive Value	(PPV)
Receiver operating characteristic	(ROC)
Region of interest	(ROI)
Short tau inversion recovery	(STIR)
Signal intensity	(SI)
Signal to noise ratio	(SNR)
Squamous cell carcinoma	(SCC)
Standardized tumor ADC	(st-ADC)
Statistical Package for Social Sciences	(SPSS)
T1-Weighted	(T1WI)
T2-Weighted MRI	(T2WI)
Transitional cell carcinoma	(TCC)
Transuretheral resection	(TUR)
Transurethral resection of bladder tumor	(TURBT)
Vesical Imaging-Reporting and Data system	(VI-RADS)
World Health Organization	(WHO)

Declarations:

Statement of Ethical Approval and Informed Consent

In accordance with the Declaration of Helsinki and the Belmont report this study was approved by the Institutional Review Board of the National Cancer Institute (IRB-NCI) (Review no. 201920032.3).

Consent for publication

All patients included in this research were above 18 years of age and gave written consent to publish the data included in the study.

Journal of Chemical Health Risks

www.jchr.org

JCHR (2025) 15(2), 1639-1655 | ISSN:2251-6727

Funding

This research did not receive any specific grant from funding agencies in the public, commercial or not-for-profit sectors. There were no sources of funding.

References

1. **Antoni S, Ferlay J, Soerjomataram I, Znaor A, Jemal A, & Bray F.** (2017). Bladder cancer incidence and mortality: a global overview and recent trends. European urology, 71(1), 96-108.

2. **Ferlay J, Soerjomataram I, Dikshit R, Eser S, Mathers C, Rebelo M, ... & Bray, F.** (2015). Cancer incidence and mortality worldwide: sources, methods and major patterns in GLOBOCAN 2012. International journal of cancer, 136(5), E359-E386.

3. **Josephson D, Pasin E & Stein JP.** (2007). Superficial bladder cancer: part 2. Management. Expert review of anticancer therapy, 7(4), 567-581.

4. **Sherif A, Jonsson MN & Wiklund NP.** (2007). Treatment of muscle-invasive bladder cancer. Expert review of anticancer therapy, 7(9), 1279-1283.

5. **Wang, H., Luo, C., Zhang, F., Guan, J., Li, S., Yao, H., ... & Guo, Y.** (2019). Multiparametric MRI for bladder cancer: validation of VI-RADS for the detection of detrusor muscle invasion. Radiology, 291(3), 668-674

6. **Barchetti G, Simone G, Ceravolo I, Salvo V, Campa R, Del Giudice F, ... & Catto JW.** (2019). Multiparametric MRI of the bladder: inter-observer agreement and accuracy with the Vesical Imaging-Reporting and Data System (VI-RADS) at a single reference center. European radiology, 1-9.

7. **Ueno Y, Takahashi S, Tamada K, et al**. Diagnostic accuracy and interobserver agreement for the Vesical Imaging-Reporting and Data System for muscle-invasive bladder cancer: a multireader validation study. Eur Urol 2019;76:54–6.

8. **Lai, A. L., & Law, Y. M. (2023).** VI-RADS in bladder cancer: Overview, pearls and pitfalls. European Journal of Radiology, 160, 110666.

9. **Panebianco V, Narumi Y, Altun E, Bochner BH, Efstathiou JA, Hafeez S., ... & Muglia VF.** (2018). Multiparametric magnetic resonance imaging for bladder cancer: development of VI-RADS (Vesical Imaging-Reporting And Data System). European urology, 74(3), 294-306.

10. **Weinreb JC, Barentsz JO, Choyke PL, Cornud F, Haider MA, Macura KJ, ... & Thoeny HC.** (2016). PI-RADS prostate imaging–reporting and data system: 2015, version 2. European urology, 69(1), 16-40.

11. **Hong, S. B., Lee, N. K., Kim, S., Son, I. W., Ha, H. K., Ku, J. Y., ... & Park, W. Y.** (2020). Vesical imaging–reporting and data system for multiparametric MRI to predict the presence of muscle invasion for bladder cancer. Journal of Magnetic Resonance Imaging, 52(4), 1249-1256

12. **Wang, Z., Shang, Y., Luan, T., Duan, Y., Wang, J., Wang, H., & Hao, J.** (2020). Evaluation of the value of the VI-RADS scoring system in assessing muscle infiltration by bladder cancer. Cancer Imaging, 20(1), 1-8.

13. **Ueno, Y., Tamada, T., Takeuchi, M., Sofue, K., Takahashi, S., Kamishima, Y., ... & Murakami, T.** (2021). VI-RADS: Multiinstitutional Multireader Diagnostic Accuracy and Interobserver Agreement Study. American Journal of Roentgenology, 216(5), 1257-1266.

14. **Vaz, A., & Zaparolli, M.** (2019). Diagnostic accuracy of retrospective application of the Vesical Imaging-Reporting and Data System: preliminary results. Radiologia brasileira, 53, 21-26.

15. **Liu, S., Xu, F., Xu, T., Yan, Y., Yao, X., & Tang, G.** (2020). Evaluation of Vesical Imaging-Reporting and Data System (VI-RADS) scoring system in predicting muscle invasion of bladder cancer. Translational andrology and urology, 9(2), 445.

16. **Ghanshyam, K., Nachiket, V., Govind, S., Shivam, P., Sahay, G. B., Mohit, S., & Ashok, K. (2022).** Validation of Vesical Imaging Reporting and Data System score for the diagnosis of muscle-invasive bladder cancer: A prospective cross-sectional study. Asian Journal of Urology, 9(4), 467-472.

17. **Makboul, M., Farghaly, S., & Abdelkawi, I. F.** (2019). Multiparametric MRI in differentiation between muscle invasive and non-muscle invasive

Journal of Chemical Health Risks
www.jchr.org
JCHR (2025) 15(2), 1639-1655 | ISSN:2251-6727

urinary bladder cancer with vesical imaging reporting and data system (VI-RADS) application. The British journal of radiology, 92(1104), 20190401.

18. **Del Giudice, F., Flammia, R. S., Pecoraro, M., Moschini, M., D'Andrea, D., Messina, E., ... & Panebianco, V.** (2022). The accuracy of Vesical Imaging-Reporting and Data System (VI-RADS): an updated comprehensive multi-institutional, multi-readers systematic review and meta-analysis from diagnostic evidence into future clinical recommendations. World Journal of Urology, 40(7), 1617-1628.

19. **Sakamoto, K., Ito, M., Ikuta, S., Nakanishi, Y., Kataoka, M., Takemura, K., ... & Koga, F.** (2020). Detection of muscle-invasive bladder cancer on biparametric MRI using vesical imaging-reporting and data system and apparent diffusion coefficient values (VI-RADS/ADC). Bladder Cancer, 6(2), 161-169.

20. Pecoraro, M., Takeuchi, M., Vargas, H. A., Muglia, V. F., Cipollari, S., Catalano, C., & Panebianco, V. (2020). Overview of VI-RADS in bladder cancer. American Journal of Roentgenology, 214(6), 1259-1268.

Figures.

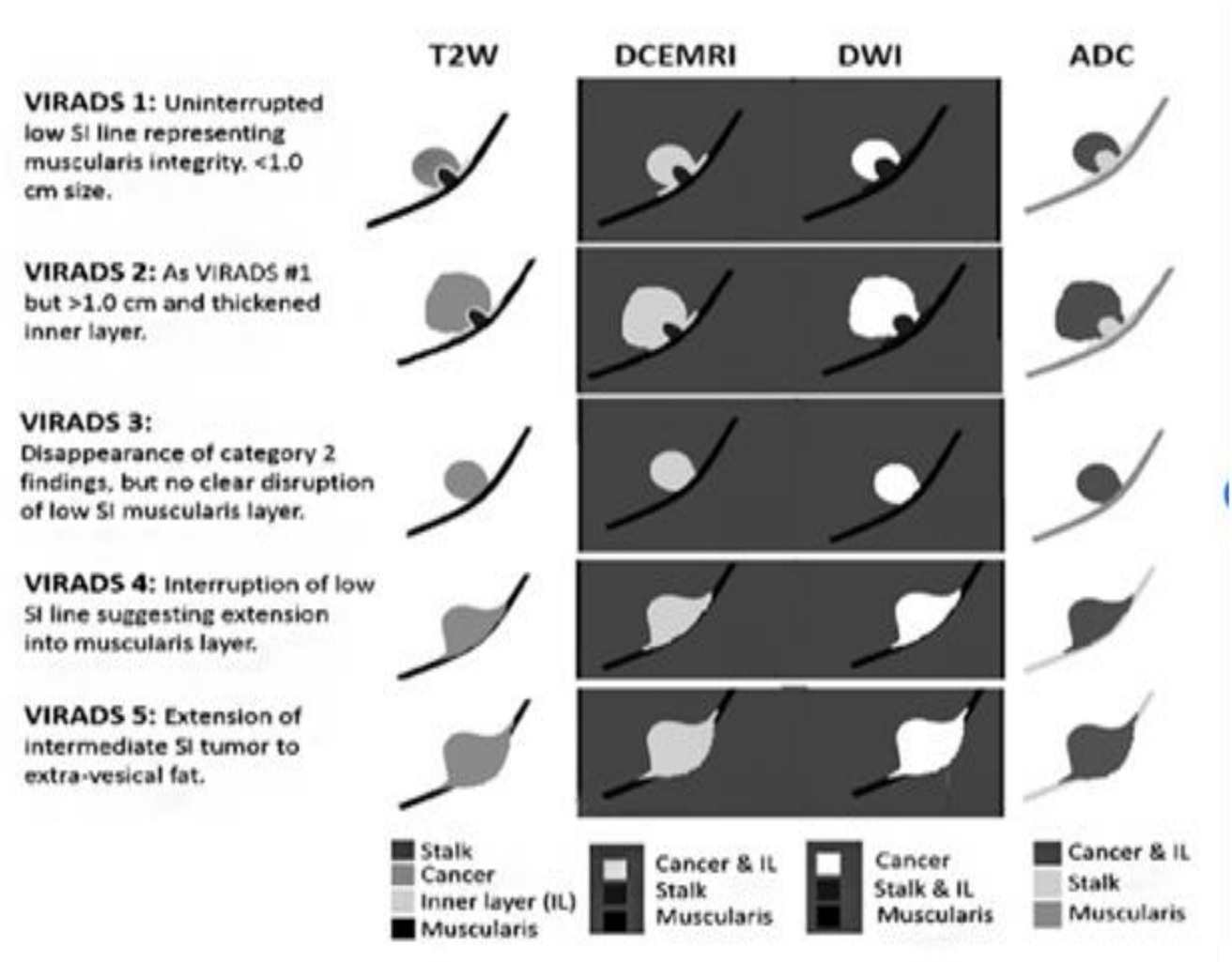

Fig. 1: Schematic illustration of mpMRI appearances of VI-RADS scores 1-5 using T2, DCE MRI, DWI, and ADC weighted images. Source: Based on Panebianco et AP and Lateral views 2018.

Journal of Chemical Health Risks
www.jchr.org
JCHR (2025) 15(2), 1639-1655 | ISSN:2251-6727

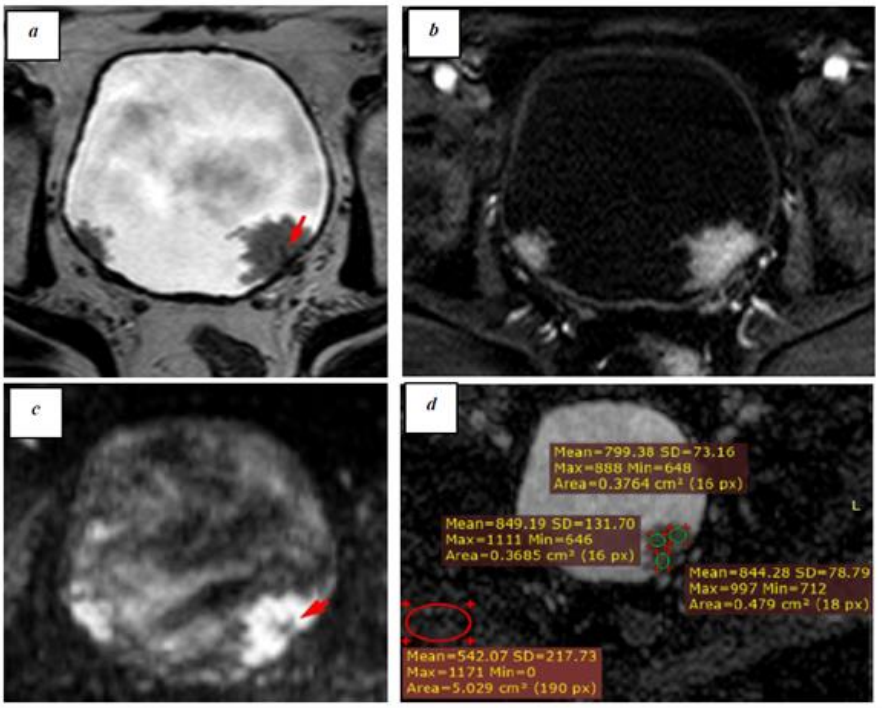

Fig. 2: Case 1: Conventional non-enhanced axial T2 WI (a), DCI (b), DWI {b values 1000} (c) and ADC map (d). Internal stalk (red arrow)

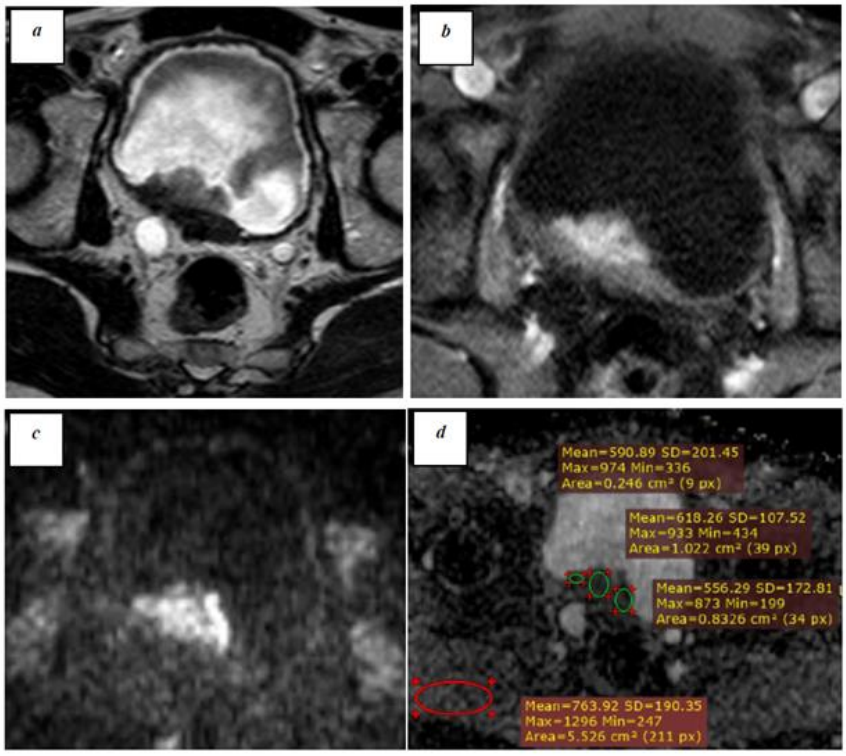

Fig. 3: Case 2: Conventional non-enhanced axial T2 WI (a), DCI (b), DWI {b values 1000} (c) and ADC map (d).

Journal of Chemical Health Risks
www.jchr.org
JCHR (2025) 15(2), 1639-1655 | ISSN:2251-6727

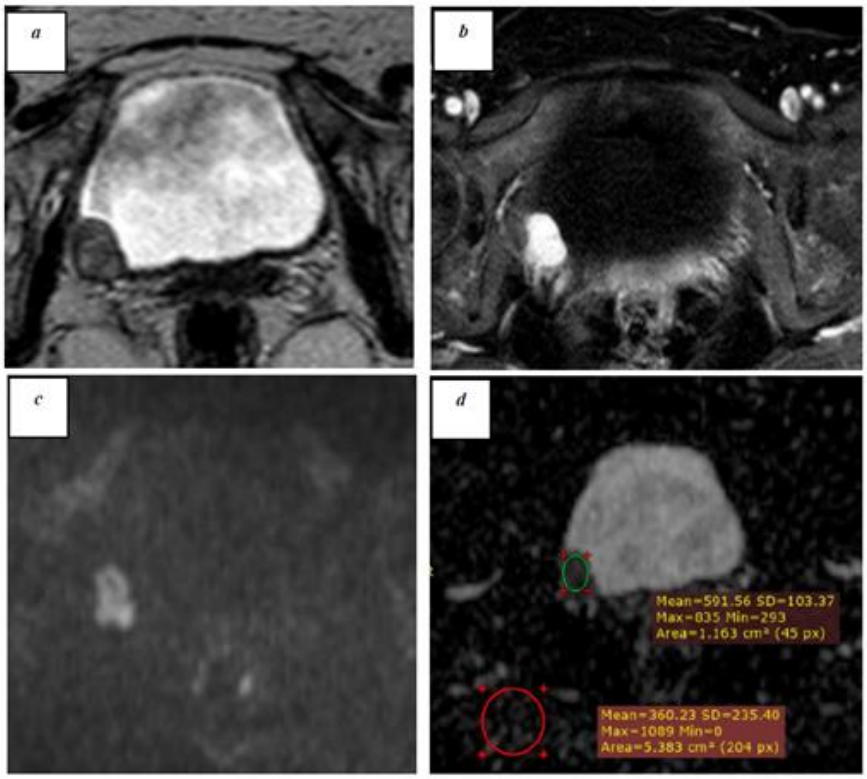

Fig. 4: Case 3: Conventional non-enhanced axial T2 WI (a), DCI (b), DWI {b values 1000} (c) and ADC map (d)

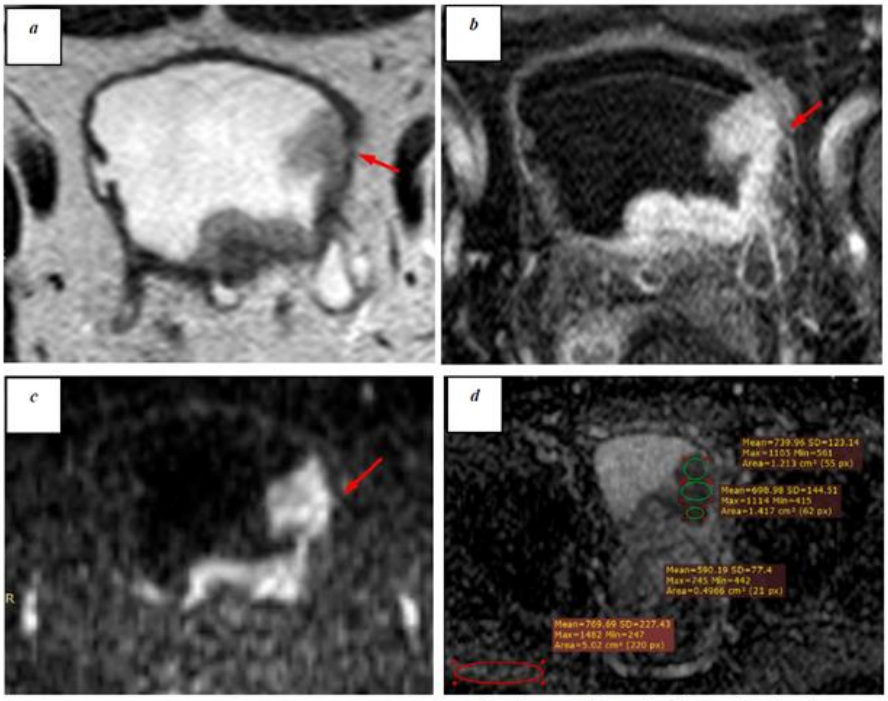

Fig. 5: Case 4: Conventional non-enhanced axial T2 WI (a), DCI (b), DWI {b values 1000} (c) and ADC map (d). Focal areas of interruption of low signal muscularis propria (red arrow)

Journal of Chemical Health Risks
www.jchr.org
JCHR (2025) 15(2), 1639-1655 | ISSN:2251-6727

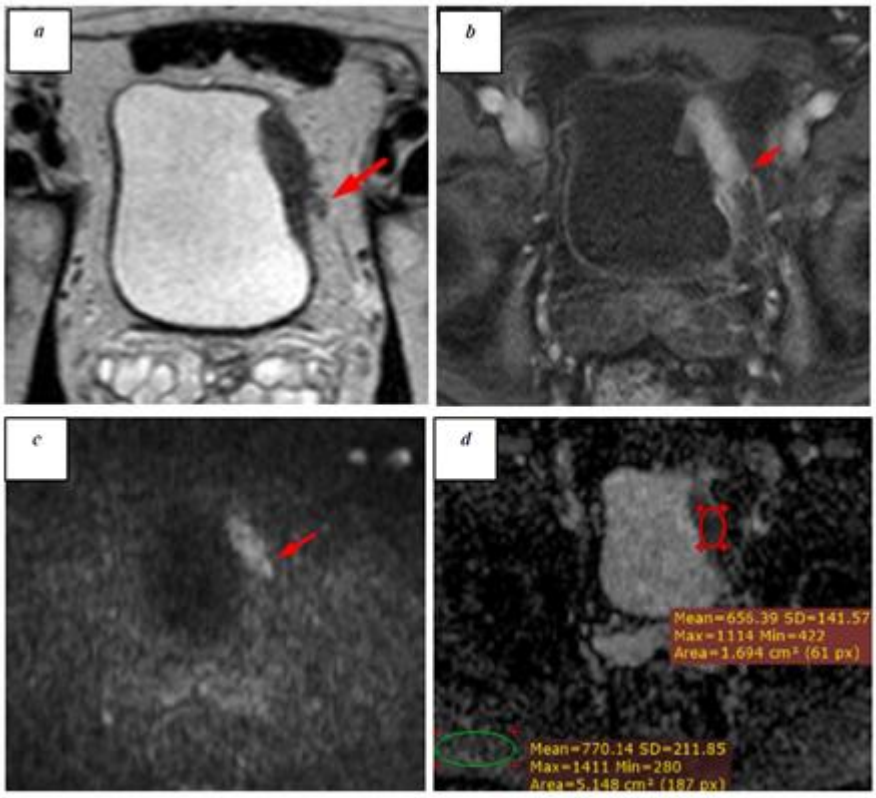

Fig. 6: Case 5: Conventional non-enhanced axial T2 WI (a), DCI (b), DWI {b values 1000} (c) and ADC map (d). Interruption of the deep muscle layer and focal area of extra-vesical extension (red arrow).

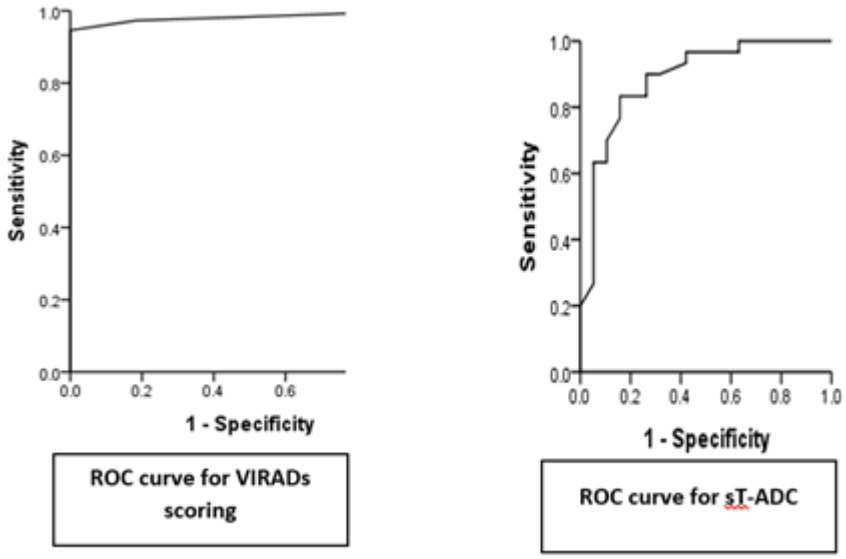

Fig. 7: ROC curves for VI-RADS scoring and sT-ADC.

Journal of Chemical Health Risks
www.jchr.org
JCHR (2025) 15(2), 1639-1655 | ISSN:2251-6727

Table 1: Summary of imaging protocol.

	T2W	DWI	DCE
TR (ms)	5352	2779	4.4
TE (ms)	115	72	2.2
Flip angle (degree)	90	90	10
FOV (cm)	26	32	27
Matrix	236 x 155	120 x 125	260 x 245
Slice thickness (mm)	3.9	3.9	1
Slice gap (mm)	0-0.4	0.3-0.4	0
Number of signal average	2-3	4-10	1
B Value (s/mm^2)		0-500-1000	

Table 2: Different MRI scores in relation to pathologic muscle invasiveness in bladder cancer patients

Imaging and Scoring System		**Pathologic muscle invasiveness**		**P Value**
		Non-muscle invasive (n = 22)	**Muscle invasive (n = 37)**	
		n (%)	**n (%)**	
Scoring T2WI	2	17 (77.3)	1 (2.7)	**< 0.001**
	3	5 (22.7)	1 (2.7)	
	4	0	6 (16.2)	
	5	0	29 (78.4)	
Scoring DWIs	2	18 (81.8)	1 (2.7)	**< 0.001**
	3	4 (18.2)	1 (2.7)	
	4	0	6 (16.2)	
	5	0	29 (78.4)	
Scoring DCE	2	18 (81.8)	1 (2.7)	**< 0.001**
	3	4 (18.2)	1 (2.7)	
	4	0	6 (16.2)	
	5	0	29 (78.4)	
Final score (VI-RADS)	2	18 (81.8)	1 (2.7)	**< 0.001**
	3	4 (18.2)	1 (2.7)	
	4	0	6 (16.2)	
	5	0	29 (78.4)	

Table 3: Diagnostic accuracy of VI-RADS scoring if cut off value ≥3

Cutoff value	**Sensitivity (%)**	**Specificity (%)**	**PPV (%)**	**NPV (%)**	**Overall accuracy (%)**	**AUC (95% CI)**	**p value**
≥3	**97.3**	**81.8**	**90.0**	**94.7**	**91.5**	**98.2 (94.7 - 1.0)**	**< 0.001**

PPV: Positive Predictive Value, NPV: Negative Predictive Value, AUC: Area under the curve, CI: Confidence Interval

Journal of Chemical Health Risks
www.jchr.org
JCHR (2025) 15(2), 1639-1655 | ISSN:2251-6727

Table 4: Diagnostic accuracy of VI-RADS scoring cut off value ≥4

Cutoff value	Sensitivity (%)	Specificity (%)	PPV (%)	NPV (%)	Overall accuracy (%)
≥4	**94.6**	**100.0**	**100.0**	**91.7**	**96.6**

Table 5: ADC and sT-ADC among the 2 pathologic groups (n= 49)			
	Pathologic muscle invasiveness		
	Muscle invasive	**Non-muscle invasive**	**p value**
	(n = 30)	**(n = 19)**	
ADC*	0.65 (0.37 - 1.70)	0.76 (0.57 - 0.99)	**<0.025**
sT-ADC*	0.77 (0.40 - 1.30)	1.06 (0.64 - 1.74)	**< 0.001**
*Data are presented as median (range)			

Table 6: Diagnostic accuracy of sT-ADC scoring

Cutoff value	Sensitivity (%)	Specificity (%)	PPV (%)	NPV (%)	Overall accuracy (%)	AUC (95% CI)	p value
<= 0.895	**83.3**	**84.2**	**89.3**	**76.2**	**83.7**	**88.8 (78.9 - 98.6)**	**< 0.001**

PPV: Positive Predictive Value, NPV: Negative Predictive Value, AUC: Area under the curve, CI: Confidence Interval

Table 7: Detectability of muscle invasion by VI-RADS, sT-ADC and VI-RADS/ADC				
Models	**Sensitivity**	**Specificity**	**PPV**	**NPV**
VI-RADS ≥3	97.3	81.8	90.0	94.7
VI-RADS ≥4	94.6	100.0	100.0	91.7
sT-ADC <= 0.895	83.3	84.2	89.3	76.2
VI-RADS/ADC				
VI-RAD ≥3 and sT-ADC <= 0.895	80.0	100.0	100.0	76.0
VI-RAD ≥3 or sT-ADC <= 0.895	100.0	68.2	84.1	100.0
VI-RAD ≥4 and sT-ADC <= 0.895	76.7	100.0	100.0	73.1